Malaysian Journal of Mathematical Sciences 7(2): 247-272 (2013)

MALAYSIAN JOURNAL OF MATHEMATICAL SCIENCES

Journal homepage: http://einspem.upm.edu.my/journal

Effect of Different Subsectional Basis and Testing Functions in the Method of Moments for the Scattering from Two Dimensional Dielectric Scatterers

[1*]Ng Tze Wei, [1,2]Zulkifly Abbas and [2]Nurul Huda Osman

[1]Institute for Mathematical Research,Universiti Putra Malaysia, 43400 UPM Serdang, Selangor, Malaysia

[2]Department of Physics, Faculty of Science, Universiti Putra Malaysia, 43400 UPM Serdang, Selangor, Malaysia

E-mail:ngwei302@gmail.com

*Corresponding author

ABSTRACT

Different integral equation formulations are reduced to a system of linear equations via method of moments (MoM) where the different basis and testing functions utilised are sinusoid/pulse, sinusoid/sinusoid, sinusoid/triangle, triangle/pulse, triangle/sinusoid and triangle/triangle methods. A hollow/layered dielectric cylinder is selected as a representative case study. Comparison is made on the convergence rate due to different testing functions where the mean relative error is investigated numerically to show the essential differences of different basis and testing functions in the MoM when different implementation techniques, boundary conditions and sizes are employed. The Gauss quadrature and staircase approximation techniques are used in calculating the impedance matrix elements. The different boundary conditions utilised are the exact and impedance boundary conditions. Numerical results point out to the need to investigate the performance of other basis and testing functions for dielectric scatterers.

Keywords: Method of moments, surface integral equation, numerical analysis, error analysis

1. INTRODUCTION

Different numerical techniques have been applied in electromagnetic problems such as the MoM for the radiation, scattering and many other applications where numerical results are verified using exact solutions, measured data, solution obtained from other techniques to provide the user confidence regarding the accuracy of the numerical solution (Davis *et al.* (2005)). Surface integral equations were developed to allow treatment of two dimensional scatterers which can be used to overcome memory size limitation needed for computer code implementation (Beker *et al.* (1990)). The continuous linear operator is projected onto finite dimensional subspaces defined by the basis and testing functions when the method of moments (MoM) is used to discretise the continuous linear equation into a matrix system to produce an approximate solution (Peterson (1998)). The choice of basis and testing functions plays a role in the accuracy and convergence of results where the theoretical convergence rates of current error and scattering error in transverse magnetic (TM) and transverse electric (TE) scattering by a circular conducting cylinder is investigated (Davis *et al.* (2004)) for different basis and testing functions. However, the effect of permittivity of dielectric object towards the convergence rate of numerical solution is not taken into account. Usually one would resort to increase the matrix size in the MoM to minimize the error in numerical computations so that this can increase the users' confidence of the numerical solution. Consequently, this result in higher computer storage requirement of the impedance matrix elements and the computation time would also increase. The effect becomes worse for large size dielectric object because the matrix size required would be very high to achieve an accurate solution.

The MoM results in fully populated matrices (Jin (2010)) and therefore the computing time and computer storage requirement is greatly increase when the matrix size is increased and this is not always desirable. When the MoM impedance matrix size has to be reduced in order to save the computer storage requirements and computation time, different basis and testing functions can result in different convergence rate when dealing with dielectric scatterers. Different implementations can give different rates of convergence and memory requirements even though the numerical technique used is the same (Jin (2010)) and this may depend on the basis and testing functions that are utilised. Hence, a comparative study on the effect of different subsectional testing functions towards the variation of error with samples/wavelength for dielectric scatterers is worthwhile because testing function that give a more acceptable result using a smaller impedance matrix size or faster convergence can be selected to save computer storage requirements and computation time.

In this paper, the different basis and testing functions considered for numerical solution are the triangle/pulse (TP), triangle/triangle (TT), triangle/sinusoid (TS), sinusoid/pulse (SP), sinusoid/triangle (ST), and sinusoid/sinusoid (SS) methods. Triangle/sinusoid refers to triangle basis sinusoid testing. These basis and testing functions are selected as the coefficients of the functions remains finite and well defined for any location of the basis and testing functions throughout the domain (Peterson (1998)). The different integral equation formulations considered in this paper are the electric field integral equation (EFIE), magnetic field integral equation (MFIE), Poggio-Muller-Chu-Harrington-Wu integral equation (PMCHW) and Muller integral equation formulations (Kishk (1991)). The different implementation techniques considered are the Gauss quadrature and staircase approximation techniques whereas the different boundary conditions selected are the exact and impedance boundary conditions.

2. THEORY

For a scatterer bounded by surface S, the scattered electric field, $\boldsymbol{E}^S$ and magnetic field, $\boldsymbol{H}^S$ generated by surface electric current, $\boldsymbol{J}$ and surface magnetic current, $\boldsymbol{M}$ on the boundary are given by (Kishk(1991))

$$\boldsymbol{E}^s(\boldsymbol{J}) = -j\omega\boldsymbol{A}(\boldsymbol{J}) - j\frac{1}{\omega\mu\epsilon}\nabla\nabla\cdot\boldsymbol{A}(\boldsymbol{J}) \quad , \tag{1}$$

$$\boldsymbol{E}^s(\boldsymbol{M}) = -\frac{1}{\epsilon}\nabla\times\boldsymbol{F}(\boldsymbol{M}) \ , \tag{2}$$

$$\boldsymbol{H}^s(\boldsymbol{J}) = \frac{1}{\mu}\nabla\times\boldsymbol{A}(\boldsymbol{J}) \ , \tag{3}$$

$$\boldsymbol{H}^s(\boldsymbol{M}) = -j\omega\boldsymbol{F}(\boldsymbol{M}) - j\frac{1}{\omega\mu\epsilon}\nabla\nabla\cdot\boldsymbol{F}(\boldsymbol{M}) \quad , \tag{4}$$

$$\boldsymbol{A}(\boldsymbol{J}) = \mu\int\boldsymbol{J}(\boldsymbol{\rho}')G(\boldsymbol{\rho},\boldsymbol{\rho}')d\boldsymbol{\rho}' \ , \tag{5}$$

$$\boldsymbol{F}(\boldsymbol{M}) = \epsilon\int\boldsymbol{M}(\boldsymbol{\rho}')G(\boldsymbol{\rho},\boldsymbol{\rho}')d\boldsymbol{\rho}' \ , \tag{6}$$

$$G(\boldsymbol{\rho},\boldsymbol{\rho}') = \frac{1}{j4}H_0^{(2)}(k|\boldsymbol{\rho}-\boldsymbol{\rho}'|) \ , \tag{7}$$

$$k = \omega\sqrt{\mu\epsilon} \quad , \tag{8}$$

$$\omega = 2\pi f \quad , \tag{9}$$

where μ is the permeability whereas ϵ is the permittivity and f is the frequency. The function $G(\boldsymbol{\rho}, \boldsymbol{\rho}')$ is the two dimensional Green's function whereas $\boldsymbol{\rho}'$ and $\boldsymbol{\rho}$ are the source and the observation points respectively. In this manuscript, the time convention $e^{j\omega t}$ is selected. According to the surface equivalence principle, piecewise homogeneous regions are replaced with equivalent electric and magnetic currents to obtain the fields in the region of interest (Kishk (1991)). To ensure the continuity of the tangential component of the fields on the interface, the surface currents on the opposite sides of the interface are taken to be of the same magnitude and in the opposite directions (Kishk (1991)). The boundary conditions are given by

$$\hat{\boldsymbol{n}} \times \boldsymbol{E}_d = 0 \text{ on } S_{cd} \, , \tag{10}$$

$$\hat{\boldsymbol{n}} \times \boldsymbol{E}_e = 0 \text{ on } S_{cf} \, , \tag{11}$$

$$\hat{\boldsymbol{n}} \times \boldsymbol{E}_d = \hat{\boldsymbol{n}} \times \boldsymbol{E}_e \text{ on } S_{df} \, , \tag{12}$$

$$\hat{\boldsymbol{n}} \times \boldsymbol{H}_d = \hat{\boldsymbol{n}} \times \boldsymbol{H}_e \text{ on } S_{df} \, , \tag{13}$$

where S_{cd} is the interface between conducting and dielectric regions. On the other hand, S_{cf} is the interface between conducting and free space region whereas S_{df} is the interface between dielectric and free space region. Equations (12) and (13) are employed as the exact boundary condition (EBC) where the equations can be replaced by the impedance boundary condition (IBC) which is given by (Kishk (1991))

$$\hat{\boldsymbol{n}} \times \boldsymbol{E} \times \hat{\boldsymbol{n}} = \eta\eta_0(\hat{\boldsymbol{n}} \times \boldsymbol{H}) \, , \tag{14}$$

$$\eta = \sqrt{\mu_r / \epsilon_r} \; . \tag{15}$$

For the details regarding the derivation of surface integral equations, one can refer to (Beker (1990)) and it will not be repeated here. The combined field integral equation is employed to avoid spurious solution due to the interior resonance problem on closed conducting and impedance surfaces (Huddleston *et al.* (1986)), (Kishk (1991)).

The different integral equation formulations are reduced to matrix system using the MoM and the general matrix takes the form $[V_m] = [Z_{mn}][I_n]$ where $[Z_{mn}]$ is the impedance matrix, $[I_n]$ is the the unknown expansion coefficients of the surface currents respectively and $[V_m]$ is the excitation matrix (Kishk (1991)). By solving the system matrix, the induced currents on all the interfaces can be determined. The generic integrals generated from MoM are given by (Gibson (2007))

$$\int f_m(\boldsymbol{\rho})\hat{\boldsymbol{z}} \cdot \boldsymbol{X}(K\hat{\boldsymbol{z}})d\boldsymbol{\rho}$$
$$= \int f_m(\boldsymbol{\rho}) \cdot \int K(\boldsymbol{\rho}')\, G(\boldsymbol{\rho},\boldsymbol{\rho}')d\boldsymbol{\rho}'d\boldsymbol{\rho} \ , \tag{16}$$

$$\int f_m(\boldsymbol{\rho})\hat{\boldsymbol{t}}\,(\boldsymbol{\rho}) \cdot \boldsymbol{X}(K\hat{\boldsymbol{t}})d\boldsymbol{\rho}$$
$$= \int f_m(\boldsymbol{\rho})\hat{\boldsymbol{t}}\,(\boldsymbol{\rho}) \cdot \int K(\boldsymbol{\rho}')\hat{\boldsymbol{t}}\,(\boldsymbol{\rho}')G(\boldsymbol{\rho},\boldsymbol{\rho}')d\boldsymbol{\rho}'d\boldsymbol{\rho} \ , \tag{17}$$

$$\int f_m(\boldsymbol{\rho})\hat{\boldsymbol{t}}\,(\boldsymbol{\rho}) \cdot \nabla\nabla \cdot \boldsymbol{X}(K\hat{\boldsymbol{t}})d\boldsymbol{\rho}$$
$$= \int f_m(\boldsymbol{\rho})\hat{\boldsymbol{t}}\,(\boldsymbol{\rho}) \cdot \nabla\nabla \cdot \int K(\boldsymbol{\rho}')\hat{\boldsymbol{t}}\,(\boldsymbol{\rho}')G(\boldsymbol{\rho},\boldsymbol{\rho}')d\boldsymbol{\rho}'d\boldsymbol{\rho} \ , \tag{18}$$

$$\int f_m(\boldsymbol{\rho})\hat{\boldsymbol{z}} \cdot \nabla \times \boldsymbol{X}(K\hat{\boldsymbol{t}})d\boldsymbol{\rho}$$
$$= \int f_m(\boldsymbol{\rho}) \int K(\boldsymbol{\rho}') \left(\hat{\boldsymbol{z}} \times \hat{\boldsymbol{t}}(\boldsymbol{\rho}')\right) \cdot \nabla' G(\boldsymbol{\rho},\boldsymbol{\rho}')d\boldsymbol{\rho}'d\boldsymbol{\rho} \ , \tag{19}$$

$$\int f_m(\boldsymbol{\rho})\hat{\boldsymbol{t}}(\boldsymbol{\rho}) \cdot \nabla \times \boldsymbol{X}(K\hat{\boldsymbol{z}})d\boldsymbol{\rho}$$
$$= \int f_m(\boldsymbol{\rho}) \int K(\boldsymbol{\rho}') \left(\hat{\boldsymbol{t}}(\boldsymbol{\rho}) \times \hat{\boldsymbol{z}}\right) \cdot \nabla' G(\boldsymbol{\rho},\boldsymbol{\rho}')d\boldsymbol{\rho}'d\boldsymbol{\rho} \ , \tag{20}$$

where $\boldsymbol{X} = \boldsymbol{A}$ or $\boldsymbol{F}$, $\boldsymbol{K} = \boldsymbol{J}$ or $\boldsymbol{M}$ and $f_m(\boldsymbol{\rho})$ is the testing function.

The singularity of generic integrals in (19) and (20) is extracted using Cauchy principal value integration before evaluating the integrals regardless of the basis and testing functions employed. When the source points coincide with the observation points, the value of the generic integrals in (19) and (20) is zero (Gibson (2007)).

$$\hat{n}(\boldsymbol{\rho}) \times \int_{\delta S^+} K(\boldsymbol{\rho}') \times \nabla' G(\boldsymbol{\rho}, \boldsymbol{\rho}') d\boldsymbol{\rho}' = K(\boldsymbol{\rho})/2 \ , \tag{21}$$

For TP and SP methods, the basis function is differentiable and the pulse testing function absorbs the derivative available in generic integral in (18) using the finite difference technique (Peterson (1998)) that is given by

$$\int f_m(\boldsymbol{\rho})\hat{\boldsymbol{t}}(\boldsymbol{\rho}) \cdot \nabla\nabla \cdot \boldsymbol{X}(K\hat{\boldsymbol{t}}) d\boldsymbol{\rho} = [\nabla \cdot \boldsymbol{X}(K\hat{\boldsymbol{t}})]_{\boldsymbol{\rho_1}}^{\boldsymbol{\rho_2}} \ , \tag{22}$$

For TT, TS, ST and SS methods, the generic integral in (18) is evaluated by distributing the del operator (Gibson (2007)) that is given by

$$\int f_m(\boldsymbol{\rho})\hat{\boldsymbol{t}}(\boldsymbol{\rho}) \cdot \nabla\nabla \cdot \boldsymbol{X}(K\hat{\boldsymbol{t}}) d\boldsymbol{\rho} = -\int \nabla \cdot [f_m(\boldsymbol{\rho})\hat{\boldsymbol{t}}(\boldsymbol{\rho})] \nabla \cdot \boldsymbol{X}(K\hat{\boldsymbol{t}}) d\boldsymbol{\rho} \ , \tag{23}$$

The singular integrals are evaluated through inner analytical integration and outer numerical integration. Details of numerical implementation can be found in (Gibson (2007)). The small argument approximation for the Hankel function is utilised when dealing with singular integrals (Gibson (2007)). The approximation employed for the Hankel function is given by

$$H_0^{(2)}(k|\boldsymbol{\rho} - \boldsymbol{\rho}'|) \cong 1 - j\frac{2}{\pi} \ln\left(\frac{\gamma k|\boldsymbol{\rho} - \boldsymbol{\rho}'|}{2}\right) \ , \tag{24}$$

where the value of γ is equal to 1.781072418.

3. METHODOLOGY

For TT, TS, ST and SS methods, the generic integrals are evaluated at 6 quadrature points for the inner and outer numerical integration over the segment with length h when the Gauss quadrature technique is employed. From Figure 1(a) and 1(b), $t_{m+1} - t_m = t_m - t_{m-1} = h$ for triangle and sinusoid testing functions whereas $t_{m+\frac{1}{2}} - t_m = t_m - t_{m-\frac{1}{2}} = h/2$ for pulse testing function. The pulse function spans from the half length of a particular segment to the half length of the adjacent segment whereas the triangle and sinusoid functions span over 2 adjacent segments. Accordingly, numerical integration for generic integrals is performed by decomposing the integrals of a particular basis function into 4 segments of the same length and each segment is evaluated over 3 quadrature points. The pulse function is decomposed into 2 segments, and each segment is evaluated over 3 quadrature points. Through that, we have maintained the same number of quadrature points for the inner and outer numerical integrations of every segment when the Gauss quadrature technique is employed.

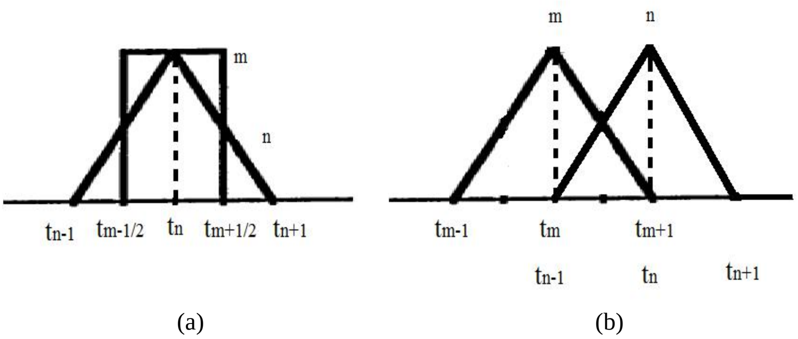

Figure 1: (a) Triangle basis and pulse testing functions (b) Triangle basis and testing functions where the *m-th* testing function overlaps with the *n-th* triangle basis function

For TT, TS, ST and SS methods, the generic integrals are evaluated using a representation of 6 pulses/intervals for the inner and outer numerical integrations over the segment with length h when the staircase approximation technique is employed. This is similar to the number of quadrature points employed in the evaluation of sinusoid and triangle functions using Gauss quadrature technique. As noted previously, the pulse function spans from the half length of a particular segment to the half length of the adjacent segment whereas the triangle and sinusoid functions span over 2 adjacent segments. Thus, numerical integration is performed by decomposing the integrals of triangle and sinusoid functions into 4 segments of the same length, and each segment is evaluated using a representation of 3 pulses/intervals. The pulse function is decomposed into 2 segments, and each segment is evaluated using a representation of 3 pulses/intervals. The number of pulses/intervals used for the pulse function in the staircase approximation technique is similar to the number of quadrature points used for the pulse function evaluated in Gauss quadrature technique.

Through that, we have maintained the same number of pulses/intervals for the inner and outer numerical integrations of every segment when the staircase approximation technique is employed. In both computing techniques, the value of the wavenumber in the sinusoid basis and testing functions is selected to be equal to the freespace wavenumber. For illustration purposes, the representation of pulse, triangle and sinusoid functions using 6 pulses/intervals over segment with length h is shown in Figure 2 where $h = t_2 - t_1$ for Figure 2(a), whereas for Figure 2(b) and Figure 2(c), $h = t_3 - t_2 = t_2 - t_1$.

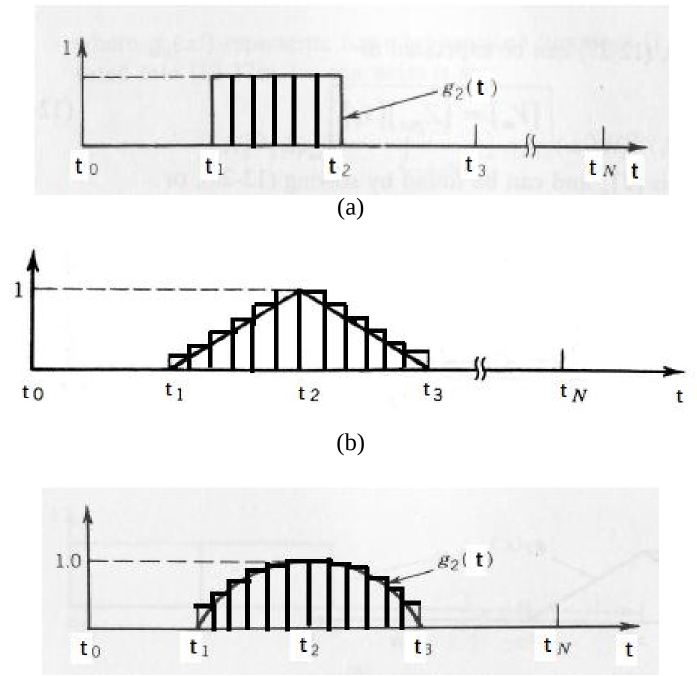

Figure 2: Staircase approximation of (a) pulse (b) triangle (c) sinusoid function using 6 pulses/intervals over segment length *h*.

In both computing techniques, the flat-faceted mesh employed is uniform where each segment is of the same length. The mesh element width is $h = \lambda/n$ where λ is the wave length of the incident plane wave and n is the number of samples/wavelength (Davis *et al.* (2005)). Comparison is made under identical solution conditions, such as the number of basis functions, the numerical integration of Green's function and similar mesh density for the different formulations. The relative error is given by

$$\delta x = \frac{\Delta x}{x} = \frac{x_0 - x}{x} , \qquad (25)$$

where x is true value of a quantity and x_0 is the calculated value of the quantity. The mean relative error of the surface current density is computed at different number of samples/wavelength.

4. VALIDATION AND VERIFICATION

To validate the computer codes, the TE scattering from a hollow dielectric cylinder with outer radius, b = (0.0819*2/π) meter and inner radius, a = (0.0819*2*0.6/π) is considered. The relative permittivity, ε_r = 4 and relative permeability μ_r = 1 at 915 MHz is selected. Due to inadequate space in the paper, only solutions for 3 angles are shown for brevity. Good agreement is observed between the exact eigenfunction series solution (Bussey *et al.* (1975)) and the MoM solution applied on the different integral equation formulations.

TABLE 1: Magnitude of the magnetic current density (unit: V/m) on the outer layer of a hollow dielectric cylinder using Gauss quadrature technique

Method	Angle(deg.)	EFIE	MFIE	PMCHW	Muller	Exact
SP	0	328.083	327.3831	328.1792	328.3338	328.1137
	90	200.0225	199.2938	200.45	200.1301	200.0712
	180	333.2926	332.9305	334.1597	333.3484	333.4593
SS	0	328.0691	327.611	328.0877	328.3244	328.1137
	90	199.9407	199.5369	200.2318	200.0557	200.0712
	180	333.3099	333.0443	333.7805	333.3951	333.4593
ST	0	328.0689	327.6109	328.0879	328.3229	328.1137
	90	199.9408	199.5368	200.2321	200.055	200.0712
	180	333.31	333.0443	333.7806	333.3945	333.4593
TP	0	328.1909	327.4925	328.2859	328.4419	328.1137
	90	200.0883	199.3611	200.5151	200.196	200.0712
	180	333.4022	333.0409	334.2682	333.458	333.4593
TS	0	328.2065	327.7206	328.0815	328.6916	328.1137
	90	200.0665	199.6044	200.202	200.4312	200.0712
	180	333.4816	333.1548	333.7958	333.8129	333.4593
TT	0	328.1768	327.7205	328.1948	328.4309	328.1137
	90	200.0066	199.6043	200.2969	200.1208	200.0712
	180	333.4197	333.1548	333.8887	333.5042	333.4593

TABLE 2: Magnitude of the magnetic current density (unit : V/m) on the outer layer of a hollow dielectric cylinder using staircase approximation technique

Method	Angle(deg.)	EFIE	MFIE	PMCHW	Muller	Exact
SP	0	328.0967	326.8061	327.7181	327.8137	328.1137
	90	199.6694	198.2682	199.5291	200.0121	200.0712
	180	333.0646	332.7043	334.2627	333.3858	333.4593
SS	0	328.1605	326.807	327.8527	327.8834	328.1137
	90	199.6267	198.2673	199.4844	199.9548	200.0712
	180	333.1116	332.7054	334.1524	333.4443	333.4593
ST	0	328.1607	326.8069	327.8523	327.8831	328.1137
	90	199.6267	198.2671	199.4853	199.954	200.0712
	180	333.1115	332.7053	334.1538	333.4434	333.4593
TP	0	328.2065	326.9164	327.8258	327.9239	328.1137
	90	199.7359	198.3356	199.5953	200.0786	200.0712
	180	333.1753	332.8159	334.3742	333.4965	333.4593
TS	0	328.2706	326.9173	327.9612	327.9936	328.1137
	90	199.6937	198.3347	199.5516	200.0213	200.0712
	180	333.223	332.817	334.2645	333.5551	333.4593
TT	0	328.2705	326.9171	327.9601	327.9933	328.1137
	90	199.6932	198.3345	199.5514	200.0204	200.0712
	180	333.2223	332.8169	334.2652	333.5541	333.4593

5. RESULTS AND DISCUSSION

The TE scattering by a hollow dielectric cylinder with outer radius, b = (0.0819*2/π) meter and inner radius, a = (0.0819*2*0.6/π) at the frequency of 915 MHz is considered. For the inner layer, ϵ_r = 1 and μ_r = 1 whilst for the outer layer, μ_r = 1 and different values of ϵ_r are selected. Numerical data in terms of the variation of outer layer surface magnetic current density mean relative error with samples/wavelength for ϵ_r = 77.3-j37.2 (Ikediala *et al*. (2002)), ϵ_r = 31.7-j136.8 (Yifen *et al.* (2003)), and ϵ_r = 75-j300 (Peterson (1994)) is tabulated in from Table 3 to Table 8 for Gauss quadrature and staircase approximation techniques. The variation of mean relative error with samples/wavelength using the Gauss quadrature technique is presented in Table 3, 4 and 5. The samples/wavelength, n used for the outer and inner radii are 30, 40, 50, 60 and 70 samples/ λ_0 where λ_0 is the free space wavelength. By taking surface electric and magnetic currents into account, these correspond to the MoM impedance matrix sizes of 96 by 96, 128 by 128, 160 by 160, 192 by 192 and 224 by 224. The computer storage requirement is denoted by the size of the matrix because the larger the matrix, the computer storage requirement needed will be higher and the computing time will increase.

The location where the testing function overlaps the basis function is the location where the source and observation points coincide. The analytical evaluation of the singular integrals using small argument approximation of the Hankel function (Gibson (2007)) would require that the length of the interval involved in the inner analytical integration of the Hankel function to be as short as possible. This is because the smaller the value of the Hankel function argument, the evaluation of the singular integrals would be more accurate. From (8), (9), and (24) the value of $|\boldsymbol{\rho} - \boldsymbol{\rho}'|$, f, μ and ϵ determine the magnitude the Hankel function argument and the parameters affect the convergence of error for the singular integrals. The width of overlapping basis and testing functions for TT, TS, SS and ST methods is higher than the TP and SP methods. The possible maximum distance between the source and observation points for the inner analytical integration of overlapping basis and testing functions due to different testing point locations of the outer numerical integration when the SP and TP methods are employed is slightly less than $h/2$. However when the SS, ST, TS and TT methods are employed, the possible maximum distance between the source and observation points for the overlapping basis and testing functions is slightly less than h.

TABLE 3: Mean relative error for hollow dielectric cylinder with ϵ_r =77.3 - j37.2 using Gauss quadrature technique

n	Equation	SP	SS	ST	TP	TS	TT
30	**EFIE**	0.0109	0.1023	0.1023	0.0137	0.1063	0.1062
	MFIE	0.0372	0.1519	0.1520	0.0341	0.1493	0.1494
	PMCHW	0.0394	0.1608	0.1609	0.0367	0.1583	0.1584
	Muller	0.0606	0.6030	0.6032	0.0643	0.6049	0.6087
40	**EFIE**	0.0052	0.0502	0.0502	0.0066	0.0523	0.0523
	MFIE	0.0184	0.0820	0.0820	0.0166	0.0803	0.0803
	PMCHW	0.0196	0.0872	0.0872	0.0182	0.0856	0.0856
	Muller	0.0270	0.2402	0.2403	0.0291	0.2414	0.2427
50	**EFIE**	0.0033	0.0284	0.0283	0.0038	0.0297	0.0296
	MFIE	0.0104	0.0488	0.0488	0.0093	0.0477	0.0477
	PMCHW	0.0113	0.0520	0.0520	0.0104	0.0509	0.0509
	Muller	0.0144	0.1260	0.1260	0.0157	0.1268	0.1274
60	**EFIE**	0.0024	0.0176	0.0176	0.0025	0.0185	0.0185
	MFIE	0.0064	0.0314	0.0314	0.0057	0.0306	0.0306
	PMCHW	0.0071	0.0334	0.0334	0.0066	0.0326	0.0326
	Muller	0.0086	0.0758	0.0758	0.0095	0.0763	0.0767
70	**EFIE**	0.0018	0.0117	0.0117	0.0018	0.0124	0.0124
	MFIE	0.0042	0.0213	0.0213	0.0037	0.0207	0.0207
	PMCHW	0.0048	0.0227	0.0227	0.0044	0.0222	0.0222
	Muller	0.0055	0.0496	0.0496	0.0062	0.0500	0.0503

TABLE 4: Mean relative error for hollow dielectric cylinder with ϵ_r = 31.7 - j136.8 using Gauss quadrature technique

n	Equation	SP	SS	ST	TP	TS	TT
30	EFIE	0.041	0.2169	0.2169	0.0429	0.2191	0.219
	MFIE	0.0391	0.1988	0.1988	0.0377	0.1978	0.1979
	PMCHW	0.0399	0.2013	0.2014	0.0388	0.2004	0.2005
	Muller	0.0988	0.4852	0.4852	0.1004	0.4867	0.4868
40	EFIE	0.0203	0.1129	0.1129	0.0214	0.114	0.114
	MFIE	0.0185	0.1064	0.1064	0.0177	0.1056	0.1057
	PMCHW	0.019	0.1078	0.1078	0.0183	0.1071	0.1071
	Muller	0.0484	0.2641	0.2642	0.0494	0.265	0.2651
50	EFIE	0.0117	0.0666	0.0666	0.0125	0.0673	0.0673
	MFIE	0.01	0.0634	0.0634	0.0095	0.0628	0.0628
	PMCHW	0.0104	0.0642	0.0642	0.01	0.0637	0.0637
	Muller	0.0277	0.1555	0.1555	0.0284	0.1561	0.1561
60	EFIE	0.0075	0.0428	0.0428	0.008	0.0433	0.0433
	MFIE	0.006	0.0408	0.0408	0.0056	0.0404	0.0404
	PMCHW	0.0062	0.0414	0.0414	0.006	0.041	0.041
	Muller	0.0175	0.0992	0.0992	0.018	0.0997	0.0997
70	EFIE	0.0051	0.0293	0.0293	0.0055	0.0297	0.0297
	MFIE	0.0038	0.0278	0.0278	0.0036	0.0275	0.0275
	PMCHW	0.004	0.0282	0.0282	0.0039	0.0279	0.0279
	Muller	0.0119	0.0674	0.0674	0.0123	0.0678	0.0678

TABLE 5: Mean relative error for hollow dielectric cylinder with ϵ_r = 75 - j300 using Gauss quadrature technique

n	Equation	SP	SS	ST	TP	TS	TT
30	EFIE	0.11	0.515	0.5151	0.112	0.5181	0.5181
	MFIE	0.1031	0.4189	0.419	0.1017	0.4183	0.4184
	PMCHW	0.1038	0.4208	0.4209	0.1025	0.4202	0.4204
	Muller	0.2663	0.8673	0.8674	0.2678	0.8688	0.8689
40	EFIE	0.0555	0.2806	0.2806	0.0566	0.2819	0.2819
	MFIE	0.0522	0.2484	0.2485	0.0513	0.2479	0.2479
	PMCHW	0.0526	0.2497	0.2498	0.0517	0.2492	0.2493
	Muller	0.1337	0.6048	0.6048	0.1346	0.6056	0.6057
50	EFIE	0.0322	0.1704	0.1704	0.033	0.1712	0.1712
	MFIE	0.0299	0.1567	0.1567	0.0293	0.1562	0.1562
	PMCHW	0.0301	0.1575	0.1576	0.0295	0.1571	0.1571
	Muller	0.0769	0.3996	0.3997	0.0775	0.4002	0.4003
60	EFIE	0.0205	0.1117	0.1117	0.0211	0.1122	0.1122
	MFIE	0.0187	0.1048	0.1048	0.0182	0.1044	0.1044
	PMCHW	0.0188	0.1053	0.1053	0.0184	0.105	0.105
	Muller	0.0486	0.2666	0.2666	0.0491	0.267	0.2671
70	EFIE	0.014	0.0774	0.0774	0.0144	0.0778	0.0778
	MFIE	0.0124	0.0735	0.0735	0.0121	0.0731	0.0731
	PMCHW	0.0125	0.0738	0.0739	0.0122	0.0735	0.0736
	Muller	0.0329	0.1848	0.1848	0.0333	0.1851	0.1851

TABLE 6: Mean relative error for hollow dielectric cylinder with ϵ_r =77.3 - j37.2 using staircase approximation technique

n	Equation	SP	SS	ST	TP	TS	TT
30	**EFIE**	0.0313	0.0316	0.0315	0.0297	0.0305	0.0304
	MFIE	0.0355	0.0356	0.0356	0.0378	0.0379	0.0379
	PMCHW	0.0425	0.0405	0.0406	0.0449	0.0429	0.0430
	Muller	0.0953	0.0960	0.0960	0.0931	0.0938	0.0938
40	**EFIE**	0.0218	0.0224	0.0223	0.0209	0.0219	0.0218
	MFIE	0.0285	0.0286	0.0286	0.0299	0.0299	0.0299
	PMCHW	0.0336	0.0322	0.0322	0.0350	0.0336	0.0336
	Muller	0.0714	0.0716	0.0716	0.0702	0.0704	0.0704
50	**EFIE**	0.0167	0.0173	0.0173	0.0162	0.0170	0.0170
	MFIE	0.0238	0.0238	0.0238	0.0247	0.0247	0.0247
	PMCHW	0.0277	0.0266	0.0267	0.0286	0.0275	0.0276
	Muller	0.0570	0.0570	0.0570	0.0562	0.0562	0.0562
60	**EFIE**	0.0135	0.0141	0.0141	0.0132	0.0139	0.0139
	MFIE	0.0204	0.0204	0.0204	0.0210	0.0210	0.0210
	PMCHW	0.0236	0.0227	0.0227	0.0242	0.0234	0.0234
	Muller	0.0474	0.0473	0.0473	0.0469	0.0468	0.0468
70	**EFIE**	0.0113	0.0119	0.0119	0.0111	0.0118	0.0118
	MFIE	0.0178	0.0178	0.0178	0.0183	0.0183	0.0183
	PMCHW	0.0205	0.0198	0.0198	0.0210	0.0203	0.0203
	Muller	0.0406	0.0405	0.0405	0.0402	0.0401	0.0401

TABLE 7: Mean relative error for hollow dielectric cylinder with ϵ_r = 31.7 - j136.8 using staircase approximation technique

n	Equation	SP	SS	ST	TP	TS	TT
30	**EFIE**	0.0429	0.0413	0.0413	0.0406	0.0394	0.0393
	MFIE	0.0494	0.0494	0.0494	0.0524	0.0525	0.0525
	PMCHW	0.0535	0.0517	0.0517	0.0566	0.0548	0.0548
	Muller	0.092	0.0896	0.0896	0.0897	0.0874	0.0874
40	**EFIE**	0.0321	0.0309	0.0308	0.0308	0.0297	0.0297
	MFIE	0.0369	0.037	0.037	0.0386	0.0387	0.0387
	PMCHW	0.0399	0.0386	0.0387	0.0416	0.0404	0.0404
	Muller	0.07	0.0681	0.0681	0.0687	0.0668	0.0668
50	**EFIE**	0.0256	0.0246	0.0246	0.0247	0.0238	0.0238
	MFIE	0.0295	0.0295	0.0295	0.0306	0.0306	0.0306
	PMCHW	0.0318	0.0309	0.0309	0.0329	0.032	0.032
	Muller	0.0565	0.0549	0.0549	0.0556	0.054	0.054
60	**EFIE**	0.0213	0.0204	0.0204	0.0207	0.0199	0.0199
	MFIE	0.0246	0.0246	0.0246	0.0253	0.0253	0.0253
	PMCHW	0.0264	0.0257	0.0257	0.0272	0.0264	0.0265
	Muller	0.0473	0.0459	0.0459	0.0467	0.0453	0.0453
70	**EFIE**	0.0182	0.0175	0.0175	0.0178	0.0171	0.0171
	MFIE	0.021	0.0211	0.0211	0.0216	0.0216	0.0216
	PMCHW	0.0226	0.022	0.022	0.0232	0.0226	0.0226
	Muller	0.0407	0.0395	0.0395	0.0403	0.0391	0.0391

TABLE 8: Mean relative error for hollow dielectric cylinder with $\epsilon_r = 75 - j300$ using staircase approximation technique

n	Equation	SP	SS	ST	TP	TS	TT
30	**EFIE**	0.0632	0.0624	0.0623	0.0611	0.0605	0.0604
	MFIE	0.0718	0.0718	0.0718	0.0746	0.0747	0.0747
	PMCHW	0.0755	0.0737	0.0737	0.0784	0.0766	0.0767
	Muller	0.1347	0.1332	0.1331	0.1325	0.131	0.131
40	**EFIE**	0.0475	0.0468	0.0468	0.0463	0.0457	0.0457
	MFIE	0.0535	0.0536	0.0535	0.0551	0.0552	0.0551
	PMCHW	0.0562	0.055	0.055	0.0578	0.0566	0.0566
	Muller	0.1035	0.1022	0.1022	0.1022	0.101	0.101
50	**EFIE**	0.038	0.0374	0.0374	0.0372	0.0367	0.0366
	MFIE	0.0427	0.0427	0.0427	0.0437	0.0437	0.0437
	PMCHW	0.0447	0.0438	0.0438	0.0457	0.0448	0.0449
	Muller	0.0839	0.0829	0.0829	0.0831	0.082	0.082
60	**EFIE**	0.0316	0.0311	0.0311	0.0311	0.0306	0.0306
	MFIE	0.0355	0.0355	0.0355	0.0362	0.0362	0.0362
	PMCHW	0.0371	0.0364	0.0364	0.0378	0.0371	0.0371
	Muller	0.0706	0.0697	0.0697	0.07	0.0691	0.0691
70	**EFIE**	0.0271	0.0266	0.0266	0.0267	0.0263	0.0262
	MFIE	0.0304	0.0304	0.0304	0.0309	0.0309	0.0309
	PMCHW	0.0317	0.0311	0.0312	0.0323	0.0317	0.0317
	Muller	0.0609	0.0601	0.0601	0.0604	0.0596	0.0596

The effect of error due to the small argument approximation of the Hankel function is not negligible for wider overlapping basis and testing functions. This is because the error due to high value of $|\boldsymbol{\rho} - \boldsymbol{\rho}'|$ from the effect of different testing point locations of the outer numerical integration is amplified by the high permittivity used in the calculation of the Hankel function wave number. Hence, under the Gauss quadrature technique the evaluation of the singular integrals would give faster convergence when SP and TP methods are employed compared to the SS, ST, TS and TT methods.

The convergence of error in the Muller integral equation formulation is slower than any other integral equation formulation when the SS, ST, TS methods are used compared to the SP and TP methods. This is because the relative permittivity is more abundant in the Muller integral equation formulation than any other integral equation formulation. Thus, the error due to the small argument approximation is intensified in a more significant degree for the Muller integral equation formulation than other integral equation formulations when a high magnitude relative permittivity is used.

For singular and non-singular integrals, the same number of computation points for every segment is applied for both computing techniques (which is quadrature points for the Gauss quadrature technique and intervals/pulses for the staircase approximation technique). The variation of outer layer surface magnetic current density mean relative error with samples/wavelength using staircase approximation technique is tabulated in Table 6, 7 and 8 by applying the same parameter value used in the Gauss quadrature technique at the frequency of 915 MHz. For the staircase approximation technique, the basis and testing functions are approximated using intervals or pulses. The evaluation of singular integrals using staircase approximation technique utilises the small argument approximation of the Hankel function for overlapping intervals/pulses of basis and testing functions (Ayyildiz, 2006).

The small argument approximation of the Hankel function is not used when the intervals/pulses do not overlap even though the basis and testing functions overlap. Thus, when dealing with overlapping basis and testing intervals or pulses, the length of the interval for the inner analytical integration of the Hankel function is maintained to be the same for all the different basis and testing functions regardless of the width of the overlapping basis and testing functions. The effect of high permittivity does not greatly affect the difference in the convergence due to different basis and testing functions for a higher number of integral equation formulations when the staircase approximation technique is employed. For this reason, the convergence due to the SP method is not distinct from the SS and ST methods and the convergence due to the TP method is not distinct from the TS and TT methods for a higher number of integral equation formulations when the staircase approximation technique is employed.

For high permittivity scatterers, it takes higher samples/wavelength for the error due to Gauss quadrature technique to be less than the error due to staircase approximation technique when the SS, ST, TS and TT methods are used compared to the SP and TP methods. A larger matrix size is required by the SS, ST, TS and TT methods than the SP and TP methods for the solutions computed using Gauss quadrature technique to be more accurate than the solutions computed using staircase approximation technique. This implies that the SS, ST, TS and TT methods are less efficient than the SP and TP methods for the Gauss quadrature technique to be more accurate than the staircase approximation technique.

The results indicate that different basis and testing functions affect the efficiency of different numerical implementations in terms of matrix size when dealing with high permittivity objects. From the numerical experimentation, if a smaller impedance matrix size is desired for large size high permittivity scatterers, the SS, ST, TS and TT methods give slower convergence rate for a higher number of integral equation formulations compared to the SP and TP methods when the Gauss quadrature technique is employed. On the other hand, when the staircase approximation technique is employed, the convergence rate due to different basis and testing functions is almost similar for a higher number of integral equation formulations even if a smaller impedance matrix size is desired for large size high permittivity scatterers.

The TE scattering by a dielectric coated impedance cylinder with outer radius, b=4/(2*π) and inner radius, a= 3/(2* π) (Kishk (1991)) at the frequency of 300 MHz is considered. For the outer layer, ϵ_r= 4 and μ_r= 1. Different sets of value are selected for the inner core. Numerical data for ϵ_r= 8-j16 and μ_r= 2-j4 (Kishk (1991)) is tabulated in Table 9. On the other hand, numerical data for ϵ_r= 12-j24 and μ_r= 3-j6 is tabulated in Table 10 whereas numerical data for ϵ_r= 16-j32 and μ_r= 4-j8 is tabulated in Table 11. For the different sets of ϵ_r and μ_r used, η = 0.25 where it is used in the impedance boundary condition (IBC) approach and numerical data is tabulated in Table 12. The IBC is used to simplify the scattering problem when the relative permittivity is large (Peterson, 1998). In order for the IBC to be valid, the fields must decay within the IBC region which must be sufficiently lossy where the absorption and attenuation of waves is influenced by the loss factor (Peterson, 1998).

The variation of outer layer magnetic current density mean relative error with samples per wavelength is tabulated in Table 9, 10, 11 and 12. The samples/wavelength selected are 30, 40, 50, 60 and 70 samples/ λ_0 where λ_0 is the free space wavelength. By taking the surface electric and magnetic currents into account, these correspond to the MoM impedance matrix sizes of 420 by 420, 560 by 560, 700 by 700, 840 by 840 and 980 by 980 under the exact boundary condition (EBC) approach. Similarly, under the impedance boundary condition (IBC) approach, these correspond to the impedance matrix sizes of 330 by 330, 440 by 440, 550 by 550, 660 by 660 and 770 by 770. Similar number of samples/wavelength is applied on the outer and inner radii of the dielectric coated impedance cylinder. The same subroutine is employed in the calculation of the generic integrals when the exact and impedance boundary conditions are imposed.

TABLE 9: Mean relative error for dielectric coated impedance cylinder with ϵ_r =8 - j16 and μ_r = 2 - j4 using Gauss quadrature technique and EBC approach

n	Equation	SP	SS	ST	TP	TS	TT
30	**EFIE**	0.018	0.0955	0.0956	0.0212	0.0983	0.099
	MFIE	0.0191	0.092	0.0921	0.0165	0.0894	0.0894
	PMCHW	0.0034	0.0083	0.0083	0.0054	0.0102	0.0104
	Muller	0.1532	0.6713	0.6715	0.1545	0.6747	0.6749
40	**EFIE**	0.0091	0.0474	0.0474	0.0108	0.0488	0.0492
	MFIE	0.0098	0.047	0.047	0.0084	0.0454	0.0454
	PMCHW	0.0027	0.0024	0.0024	0.0037	0.0036	0.0038
	Muller	0.0771	0.3741	0.3742	0.0777	0.3755	0.3756
50	**EFIE**	0.0057	0.0273	0.0273	0.0067	0.0282	0.0284
	MFIE	0.006	0.0275	0.0275	0.0052	0.0265	0.0265
	PMCHW	0.0024	0.0019	0.0019	0.003	0.0026	0.0026
	Muller	0.0449	0.2276	0.2277	0.0453	0.2284	0.2284
60	**EFIE**	0.0041	0.0173	0.0174	0.0048	0.0179	0.0181
	MFIE	0.0043	0.0177	0.0177	0.0037	0.017	0.017
	PMCHW	0.0023	0.002	0.002	0.0027	0.0025	0.0024
	Muller	0.0289	0.1486	0.1486	0.0292	0.149	0.149
70	**EFIE**	0.0033	0.0118	0.0118	0.0038	0.0122	0.0124
	MFIE	0.0034	0.0122	0.0122	0.003	0.0117	0.0117
	PMCHW	0.0023	0.0021	0.0021	0.0025	0.0024	0.0024
	Muller	0.0201	0.1025	0.1025	0.0203	0.1028	0.1028

TABLE 10: Mean relative error for dielectric coated impedance cylinder with ϵ_r =12 - j24 and μ_r = 3 - j6 using Gauss quadrature technique and EBC approach

n	Equation	SP	SS	ST	TP	TS	TT
30	**EFIE**	0.048	0.2558	0.256	0.0512	0.2591	0.2599
	MFIE	0.0485	0.2301	0.2302	0.0457	0.228	0.2281
	PMCHW	0.0046	0.0607	0.0607	0.0069	0.0627	0.063
	Muller	0.5226	1.6528	1.6531	0.5251	1.6596	1.6598
40	**EFIE**	0.0236	0.1272	0.1272	0.0254	0.1288	0.1292
	MFIE	0.0245	0.1208	0.1208	0.0229	0.1194	0.1194
	PMCHW	0.0027	0.0159	0.0159	0.0039	0.0171	0.0172
	Muller	0.2815	1.0906	1.0908	0.2825	1.0934	1.0935
50	**EFIE**	0.0137	0.0739	0.0739	0.0148	0.0749	0.0751
	MFIE	0.0144	0.0721	0.0721	0.0134	0.0711	0.0711
	PMCHW	0.0024	0.006	0.006	0.0031	0.0067	0.0068
	Muller	0.1684	0.7376	0.7377	0.1689	0.7389	0.739
60	**EFIE**	0.0088	0.0473	0.0473	0.0096	0.0479	0.0481
	MFIE	0.0094	0.0468	0.0468	0.0087	0.0461	0.0461
	PMCHW	0.0023	0.0031	0.0031	0.0027	0.0036	0.0036
	Muller	0.1091	0.5151	0.5151	0.1094	0.5158	0.5158
70	**EFIE**	0.0062	0.0323	0.0323	0.0068	0.0328	0.0329
	MFIE	0.0067	0.0324	0.0324	0.0062	0.0318	0.0318
	PMCHW	0.0023	0.0022	0.0022	0.0025	0.0025	0.0026
	Muller	0.0752	0.3715	0.3715	0.0754	0.3719	0.3719

TABLE 11: Mean relative error for dielectric coated impedance cylinder with ϵ_r =16 - j32 and μ_r = 4 - j8 using Gauss quadrature technique and EBC approach

n	Equation	SP	SS	ST	TP	TS	TT
30	**EFIE**	0.0968	0.5234	0.5238	0.1002	0.5276	0.5285
	MFIE	0.0942	0.4294	0.4296	0.0915	0.4281	0.4283
	PMCHW	0.0111	0.24	0.2402	0.0134	0.2425	0.2429
	Muller	1.0955	2.5076	2.5079	1.1	2.5177	2.5177
40	**EFIE**	0.0479	0.257	0.2571	0.0497	0.2588	0.2593
	MFIE	0.048	0.2311	0.2312	0.0464	0.2299	0.23
	PMCHW	0.004	0.0627	0.0627	0.0053	0.0638	0.0639
	Muller	0.6528	1.9083	1.9086	0.6545	1.9127	1.9129
50	**EFIE**	0.0277	0.1491	0.1491	0.0288	0.1501	0.1504
	MFIE	0.0282	0.1402	0.1403	0.0272	0.1393	0.1394
	PMCHW	0.0026	0.0223	0.0223	0.0033	0.023	0.023
	Muller	0.4128	1.4364	1.4366	0.4136	1.4386	1.4387
60	**EFIE**	0.0176	0.0957	0.0957	0.0184	0.0964	0.0965
	MFIE	0.0182	0.0922	0.0922	0.0175	0.0916	0.0916
	PMCHW	0.0023	0.0098	0.0098	0.0027	0.0103	0.0103
	Muller	0.2759	1.0862	1.0863	0.2764	1.0874	1.0875
70	**EFIE**	0.0121	0.0657	0.0657	0.0126	0.0662	0.0663
	MFIE	0.0126	0.0643	0.0643	0.0121	0.0638	0.0638
	PMCHW	0.0023	0.0052	0.0052	0.0025	0.0056	0.0056
	Muller	0.1934	0.831	0.8311	0.1937	0.8317	0.8318

TABLE 12: Mean relative error for dielectric coated impedance cylinder using Gauss quadrature technique and IBC approach

n	Equation	SP	SS	ST	TP	TS	TT
30	**EFIE**	0.0118	0.0109	0.0109	0.0093	0.0094	0.0094
	MFIE	0.0113	0.0115	0.0115	0.0087	0.0092	0.0092
	PMCHW	0.0112	0.0114	0.0115	0.0086	0.0089	0.0089
	Muller	0.0108	0.0099	0.0099	0.0082	0.0087	0.0088
40	**EFIE**	0.0117	0.0104	0.0104	0.0103	0.0092	0.0092
	MFIE	0.0114	0.0111	0.0111	0.01	0.0096	0.0096
	PMCHW	0.0113	0.0113	0.0113	0.0099	0.0098	0.0098
	Muller	0.0112	0.0102	0.0102	0.0097	0.009	0.0089
50	**EFIE**	0.0117	0.0109	0.0109	0.0108	0.0101	0.01
	MFIE	0.0115	0.0113	0.0113	0.0106	0.0103	0.0103
	PMCHW	0.0115	0.0114	0.0114	0.0105	0.0105	0.0104
	Muller	0.0114	0.0108	0.0108	0.0104	0.01	0.0099
60	**EFIE**	0.0117	0.0112	0.0112	0.0111	0.0106	0.0105
	MFIE	0.0116	0.0114	0.0114	0.0109	0.0107	0.0107
	PMCHW	0.0115	0.0115	0.0115	0.0109	0.0108	0.0108
	Muller	0.0115	0.0112	0.0112	0.0108	0.0106	0.0105
70	**EFIE**	0.0117	0.0113	0.0113	0.0113	0.0109	0.0109
	MFIE	0.0116	0.0115	0.0115	0.0111	0.011	0.011
	PMCHW	0.0116	0.0116	0.0116	0.0111	0.0111	0.0111
	Muller	0.0115	0.0114	0.0114	0.0111	0.0109	0.0109

Under the exact boundary condition (EBC) approach, the EBC is applied on the outer layer and the core of the dielectric coated impedance cylinder whilst under the impedance boundary condition (IBC) approach, the IBC is applied only on the inner core and the EBC is applied on the outer layer of the dielectric coated impedance cylinder (Kishk (1991)). Thus, the governing integral equations using the EBC and IBC approaches are only different at the core of the dielectric coated impedance cylinder. When the EBC approach is employed, the relative permittivity and permeability of the core is used in the calculation of Hankel function. As a result, SP and TP methods give faster convergence than the SS, ST, TS and TT methods. Under the EBC approach, the difference in the convergence due to different basis and testing functions for the PMCHW integral equation formulation is not as distinct as the EFIE and MFIE formulations. This is because the equations governing the interior and exterior regions are separated in the EFIE and MFIE formulations whereas the equations are coupled in the PMCHW integral equation formulation. The effect of small argument approximation of the Hankel function is dampen in the PMCHW integral equation formulation compared to the EFIE and MFIE integral equation formulations.

For the PMCHW integral equation formulation, only two governing integral equations on the core of the dielectric coated impedance cylinder under the EBC approach that are affected by the error due to the small argument approximation of the Hankel function. This is in contrast with four governing equations on the core and outer layer in the case of the high permittivity hollow dielectric cylinder considered previously in Table 3, 4, and 5 since the location of high permittivity is in the core and not on the outer layer of the dielectric coated impedance cylinder. Though integral equations governing the interior and exterior regions are coupled in the Muller integral equation formulation, the value of the relative permittivity and permeability is abundant in the formulation where this intensifies the error due to the small argument approximation of the Hankel function. Hence, the difference in the convergence due to different basis and testing functions for the formulation is more distinct compared to the PMCHW integral equation formulation when the EBC approach is employed.

When the IBC approach is employed, the relative permittivity and permeability of the core is not used in the calculation of the Hankel function argument and it is only used for the calculation of the surface impedance given by equation (15). As a result, the difference in the convergence due to different basis and testing functions under the IBC approach is not as distinct as under the EBC approach which can be clearly observed for the Muller integral equation formulation. The error due to the small argument approximation of the Hankel function is amplified by the abundant relative permittivity and permeability when the EBC approach is employed whilst under the IBC approach, the difference in the convergence due to different basis and testing functions for the Muller integral equation formulation is almost negligible.

The difference in the convergence due to different basis and testing functions for the highly lossy dielectric coated impedance cylinder under the IBC approach is not as distinct as under the EBC approach for a higher number of integral equation formulations. The results imply that the surface impedance, η utilised in the IBC approach does not greatly affect the difference in the convergence due to different basis and testing functions even though the relative permittivity and permeability utilised for the core is quite high. This indicate that any of the basis and testing functions can be selected under the IBC approach although the SP and TP methods converge faster than the SS, ST, TS and TT methods under the EBC approach.

The scattering from two different sizes of hollow dielectric cylinders is considered. For the small size cylinder, outer radius b = (0.0819*2/π) m and inner radius a = (0.0819*2*0.6/π) m is selected whereas for the large size cylinder, outer radius b = (0.0819*2*2/π) m and inner radius a = (0.0819*2*2*0.6/π) m is selected. The dielectric media with ε_r = 54.2-j61.3 (Yifen, et al., 2003) and ε_r = 75.7-j67.1 at 915 MHz is considered (Ikediala et al., 2002) where the samples per wavelength selected are 50, 60, 70, 80 and 90 samples/λ_0. These correspond to impedance matrix sizes of 160 by 160, 192 by 192, 224 by 224, 256 by 256 and 288 by 288 respectively for the small size object whereas for the large size object, these correspond to impedance matrix sizes of 320 by 320, 384 by 384, 448 by 448, 512 by 512 and 576 by 576 respectively. For the small size object, the impedance matrix sizes of 160 by 160, 192 by 192, 224 by 224, 256 by 256 and 288 by 288 correspond to 25600, 36864, 50176, 65536 and 82944 matrix elements respectively. For the large size object, the impedance matrix sizes of 320 by 320, 384 by 384, 448 by 448, 512 by 512 and 576 by 576 correspond to 102400, 147456, 200704, 262144 and 331776 matrix elements respectively. The variation of outer layer magnetic current density mean relative error with samples per wavelength is tabulated in Table 13, 14, 15 and 16.

TABLE 13: Mean relative error for small size hollow dielectric cylinder with ϵ_r =54.2 - j61.3 using Gauss quadrature technique

n	Equation	SP	SS	ST	TP	TS	TT
50	**EFIE**	0.0074	0.0343	0.0343	0.0085	0.0356	0.0356
	MFIE	0.0088	0.0373	0.0373	0.0077	0.0362	0.036
	PMCHW	0.0086	0.0404	0.0404	0.0076	0.0394	0.0392
	Muller	0.0249	0.1739	0.174	0.026	0.1757	0.1754
60	**EFIE**	0.0046	0.0215	0.0215	0.0054	0.0224	0.0224
	MFIE	0.0062	0.0242	0.0242	0.0054	0.0234	0.0233
	PMCHW	0.0058	0.0261	0.0261	0.0051	0.0254	0.0253
	Muller	0.0147	0.1052	0.1053	0.0155	0.1064	0.1062
70	**EFIE**	0.0031	0.0145	0.0145	0.0036	0.0151	0.0151
	MFIE	0.0046	0.0167	0.0167	0.004	0.0161	0.016
	PMCHW	0.0042	0.018	0.0179	0.0037	0.0174	0.0173
	Muller	0.0093	0.0692	0.0692	0.0099	0.07	0.0698
80	**EFIE**	0.0022	0.0102	0.0102	0.0026	0.0107	0.0107
	MFIE	0.0036	0.0121	0.0121	0.0032	0.0117	0.0116
	PMCHW	0.0032	0.0129	0.0129	0.0028	0.0125	0.0124
	Muller	0.0062	0.0481	0.0481	0.0066	0.0488	0.0486
90	**EFIE**	0.0016	0.0075	0.0075	0.0019	0.0079	0.0079
	MFIE	0.0029	0.0091	0.0091	0.0026	0.0087	0.0087
	PMCHW	0.0025	0.0097	0.0097	0.0022	0.0093	0.0093
	Muller	0.0043	0.035	0.035	0.0046	0.0355	0.0354

TABLE 14: Mean relative error for large size hollow dielectric cylinder with ϵ_r =54.2 - j61.3 using Gauss quadrature technique

n	Equation	SP	SS	ST	TP	TS	TT
50	**EFIE**	0.0064	0.0364	0.0364	0.0076	0.0377	0.0377
	MFIE	0.0098	0.0354	0.0353	0.0087	0.0342	0.0341
	PMCHW	0.0064	0.0352	0.0352	0.0054	0.0341	0.0341
	Muller	0.0514	0.35	0.35	0.0523	0.3513	0.3514
60	**EFIE**	0.0039	0.0228	0.0228	0.0047	0.0237	0.0237
	MFIE	0.0072	0.023	0.0229	0.0064	0.0221	0.0221
	PMCHW	0.0042	0.0226	0.0226	0.0035	0.0218	0.0218
	Muller	0.0307	0.2148	0.2148	0.0313	0.2156	0.2157
70	**EFIE**	0.0025	0.0153	0.0153	0.0031	0.016	0.016
	MFIE	0.0056	0.0159	0.0159	0.0051	0.0152	0.0152
	PMCHW	0.0029	0.0154	0.0154	0.0024	0.0148	0.0148
	Muller	0.0197	0.142	0.142	0.0201	0.1426	0.1426
80	**EFIE**	0.0017	0.0108	0.0108	0.0022	0.0113	0.0113
	MFIE	0.0046	0.0116	0.0115	0.0042	0.0111	0.011
	PMCHW	0.0022	0.011	0.011	0.0018	0.0106	0.0106
	Muller	0.0133	0.0992	0.0992	0.0136	0.0996	0.0996
90	**EFIE**	0.0013	0.0079	0.0079	0.0016	0.0083	0.0083
	MFIE	0.0039	0.0087	0.0087	0.0035	0.0084	0.0083
	PMCHW	0.0017	0.0082	0.0082	0.0014	0.0078	0.0078
	Muller	0.0093	0.0722	0.0722	0.0095	0.0725	0.0725

TABLE 15: Mean relative error for small size hollow dielectric cylinder with ϵ_r =75.7 - j67.1 using Gauss quadrature technique

n	Equation	SP	SS	ST	TP	TS	TT
50	EFIE	0.0076	0.0442	0.0442	0.0088	0.0456	0.0456
	MFIE	0.0116	0.0513	0.0512	0.0104	0.0502	0.05
	PMCHW	0.0113	0.0532	0.0532	0.0101	0.0521	0.0519
	Muller	0.03	0.2252	0.2252	0.0313	0.2271	0.2268
60	EFIE	0.0046	0.0277	0.0277	0.0054	0.0287	0.0287
	MFIE	0.0079	0.0334	0.0333	0.0071	0.0326	0.0325
	PMCHW	0.0076	0.0346	0.0345	0.0068	0.0338	0.0337
	Muller	0.0177	0.1348	0.1348	0.0185	0.136	0.1358
70	EFIE	0.003	0.0186	0.0186	0.0036	0.0193	0.0193
	MFIE	0.0058	0.023	0.023	0.0052	0.0225	0.0224
	PMCHW	0.0054	0.0238	0.0238	0.0048	0.0232	0.0231
	Muller	0.0111	0.0881	0.0881	0.0117	0.0889	0.0888
80	EFIE	0.0021	0.0131	0.0131	0.0025	0.0136	0.0136
	MFIE	0.0045	0.0166	0.0166	0.004	0.0162	0.0161
	PMCHW	0.0041	0.0172	0.0171	0.0036	0.0167	0.0166
	Muller	0.0073	0.0611	0.0611	0.0078	0.0617	0.0617
90	EFIE	0.0015	0.0095	0.0095	0.0018	0.01	0.01
	MFIE	0.0036	0.0125	0.0125	0.0032	0.0121	0.0121
	PMCHW	0.0032	0.0128	0.0128	0.0028	0.0125	0.0124
	Muller	0.005	0.0443	0.0443	0.0054	0.0448	0.0447

TABLE 16: Mean relative error for large size hollow dielectric cylinder with ϵ_r =75.7 - j67.1 using Gauss quadrature technique

n	Equation	SP	SS	ST	TP	TS	TT
50	EFIE	0.0081	0.0485	0.0485	0.0095	0.0498	0.0498
	MFIE	0.0118	0.0465	0.0464	0.0106	0.0452	0.0452
	PMCHW	0.0084	0.046	0.046	0.0073	0.0449	0.0449
	Muller	0.075	0.5207	0.5208	0.076	0.5223	0.5225
60	EFIE	0.0049	0.0305	0.0305	0.0058	0.0314	0.0314
	MFIE	0.0084	0.0302	0.0302	0.0076	0.0293	0.0293
	PMCHW	0.0054	0.0296	0.0296	0.0046	0.0288	0.0288
	Muller	0.0448	0.317	0.317	0.0455	0.3179	0.318
70	EFIE	0.0032	0.0205	0.0205	0.0038	0.0212	0.0212
	MFIE	0.0064	0.0209	0.0209	0.0059	0.0202	0.0202
	PMCHW	0.0038	0.0203	0.0203	0.0032	0.0197	0.0197
	Muller	0.0288	0.2082	0.2082	0.0293	0.2088	0.2089
80	EFIE	0.0022	0.0145	0.0145	0.0027	0.015	0.015
	MFIE	0.0052	0.0151	0.0151	0.0047	0.0146	0.0146
	PMCHW	0.0028	0.0145	0.0145	0.0023	0.014	0.014
	Muller	0.0195	0.1448	0.1448	0.0198	0.1452	0.1452
90	EFIE	0.0015	0.0106	0.0106	0.0019	0.011	0.011
	MFIE	0.0043	0.0114	0.0114	0.004	0.011	0.011
	PMCHW	0.0021	0.0108	0.0108	0.0018	0.0104	0.0104
	Muller	0.0137	0.1051	0.1051	0.014	0.1054	0.1054

For the high permittivity hollow dielectric cylinder, the different integral equation formulations are governed by two surface electric current densities and two surface magnetic current densities. Two integral equations in the EFIE and MFIE formulations and also four integral equations in the PMCHW and Muller integral equation formulations are affected by the error due to the small argument approximation of the Hankel function. The inner layer surface current densities are affected by the error due to the small argument approximation of the Hankel function for the equations of the inner layer. The error intensified by the high relative permittivity and this slows down the convergence of the outer layer surface current densities.

In addition to that, the outer layer surface current densities are affected by the error due to the small argument approximation of the Hankel function through the equations on the outer layer. The error is intensified by the high relative permittivity and this slows down the convergence of the outer layer surface current densities. As a result, the mesh element size has to be small by taking a significantly large number of segmentations for the outer and inner layers of the hollow dielectric cylinder with large size to minimize the error due to the small argument approximation of the Hankel function. By increasing the outer and inner radii of the high permittivity hollow dielectric cylinder, the impedance matrix size utilised for the surface electric and magnetic current densities had to be increased significantly to minimize the error of the numerical solutions.

The numerical results imply that when the size of the hollow dielectric cylinder is large by increasing the inner and outer radii, the SP and TP methods still provide faster convergence than the SS, ST, TS and TT methods. A higher difference in the number of matrix elements between the SS, ST and SP methods and also between the TS, TT and TP methods to achieve an error less than 0.01 or 1% is observed for the large size object. When the size of the high permittivity hollow dielectric cylinder is small by having a smaller inner and outer radii, the SP and TP methods still provide faster convergence than the SS, ST, TS and TT methods. A smaller difference in the number of matrix elements between the SS, ST and SP methods and also between the TS, TT and TP methods to achieve an error less than 0.01 or 1% is observed for the small size object. This indicate that the efficiency of the numerical solutions in terms of memory requirements denoted by the number of matrix elements to achieve an error less than 0.01 for the SS, ST, TS and TT methods will be significantly different than the SP and TP methods as the size of the high permittivity object is increased.

It can be deduced that the amount of difference in the number of impedance matrix elements between SS, ST and SP methods and also between TS, TT and TP methods to achieve an error less than 0.01 depends on the size of the high permittivity object. From the numerical experimentation, a larger difference in the efficiency in terms of the number of matrix elements is observed between the SS, ST and SP methods and also between the TS, TT and TP methods to achieve an error less than 0.01 for large size object compared to the small size object. When the size of the high permittivity object is smaller, this leads to a smaller difference in the efficiency in terms of number of impedance matrix elements between the SS, ST and SP methods and also between the TS, TT and TP methods to achieve an error less than 0.01. Higher difference in the number of matrix elements between the different basis and testing functions in minimizing the error denotes a higher difference in the memory usage in minimizing the error of the numerical solution.

6. CONCLUSION

Different basis and testing functions are applied on different integral equation formulations where different numerical implementations, boundary conditions and sizes are considered. The convergence of different integral equation formulations using different testing functions is compared when the integral equation formulations are applied on two dimensional dielectric objects. Numerical results for the MoM surface integral equations using different basis and testing functions on dielectric objects indicate that different computing techniques and boundary conditions can result in different convergence rate when different basis and testing functions are employed as the MoM impedance matrix size is reduced to save memory requirements and computing time.

REFERENCES

Ayyildiz, K. 2006. Surface Integral Solution of Chiral Loaded Waveguides of Arbitrary Cross Section, Ph.D Thesis, Sycrause University, US.

Beker, B., Umashankar, K. R. and Taflove, A. 1990. Electromagnetic Scattering by Arbitrarily Shaped Two-Dimensional Perfectly Conducting Objects Coated with Homogeneous Anisotropic Materials. *Electromagnetics*. **10**(4):387-406.

Bussey, H. E. and Richmond, J. H. 1975. Scattering by a Lossy Dielectric Circular Cylindrical Multilayer, Numerical Values. *IEEE Trans. Antennas Propagat.* **23**(5):723- 725.

Davis, C. P. and Warnick, K. F. 2004. Higher-Order Convergence With Low Order Discretisation of the 2D-MFIE. *IEEE Antennas Wireless Propagat. Letters.* **3**(1):355-358.

Davis, C. P. and Warnick, K. F. 2005. Error Analysis of 2-D MoM for MFIE/EFIE/CFIE based on the Circular Cylinder. *IEEE Trans. Antennas Propagat.* **53**(1):321-331.

Gibson, W. C. 2007. *The Method of Moments in Electromagnetics*. Boca Raton: Chapman and Hall/CRC.

Huddleston, P. L., Medgyesi–Mitschang, L. N. and Putnam, J. M. 1986 Combined Field Integral Equation Formulation for Scattering by Dielectrically Coated Conducting Bodies. *IEEE Trans. Antennas Propagat.* **34**(4):510-520.

Ikediala, J. N., Hansen, J. D., Tang, J., Drake, S. R. and Wang, S. 2002. Development of a saline water immersion technique with RF energy as a postharvest treatment against codling moth in cherries. *Postharvest Biology and Technology.* **24**(2):209-221.

Jin, J. M. 2010. *Theory and Computation of Electromagnetic Fields*. John Wiley and Sons.

Kishk, A. A. 1991. Electromagnetic Scattering from Composite Objects Using a Mixture of Exact and Impedance Boundary Conditions. *IEEE Trans. Antennas Propagat.* **39**(6):826-833.

Kishk, A. A., Glisson, A. W., Goggans, P. M. 1992. Scattering from Conductors Coated with Materials of Arbitrary Thickness. *IEEE Trans. Antennas Propagat.* **40**(1):108-112.

Peterson, A. F. 1994. Application of volume discretisation methods to oblique scattering from high contrast penetrable cylinders. *IEEE Trans. Microwave Theory and Techniques*. **42**(4):686-689.

Peterson, A. F., Ray, S. L. and Mittra, R. 1998. *Computational Methods for Electromagnetics*. New York: IEEE Press.

Yifen, W., Timothy, D. W., Juming, T. and Linnea, M. H. 2003. Dielectric properties of foods relevant to RF and microwave pasteurization and sterilization. *Journal of Food Engineering.* **57**:257–268.